# Supplementary Information

## The opening/closure of P-loop and hinge of BCR-ABL1 decodes the low/high bioactivities of dasatinib and axitinib

Jianyi Wang, [a] Qing Chen,[a] Mian Wang*[ab] and Cheng Zhong[c]

[a]School of Chemistry and Chemical Engineering, Guangxi University, Nanning 530004, China
[b]College of Life Science and Technology, Guangxi University, Nanning 530004, China *E-mail: mianwang@gxu.edu.cn
[c]School of Computer, Electronics and Information, Guangxi University, Nanning 530004, China

The initial structure of dasatinib:BCR-ABL1(WT) complex where BCR-ABL1 adopted the DFG-in conformation was obtained from protein data bank (pdb code 2GQG). To comparatively describe the conformation change of DFG-in conformational BCR-ABL(WT) caused by axitinib, the initial structure of axitinib:BCR-ABL1(WT) was generated through replacing dasatinib by axitinib in the crystal structure of the dasatinib:BCR-ABL1(WT) complex when superposing the crystal structures of dasatinib:BCR-ABL1(WT) (pdb code 2GQG) and axitinib:BCR-ABL1(WT) (pdb code 4WA9). The initial structures of dasatinib:BCR-ABL1(T315I) and axitinib:BCR-ABL1(T315I), where kinases adopt DFG-in conformations, were obtained through changing threonine 315 of the above dasatinib:BCR-ABL1(WT) and axitinib:BCR-ABL1(WT) complexes into isoleucine with chimera software. There are no steric clashes between ligand and protein in the above four systems. The missing residues were repaired using modeller 9.0. These initial structures were subjected to molecular dynamics simulations using GROMACS 4.5.5 package. The binding free energy was calculated with the MM-PBSA method.

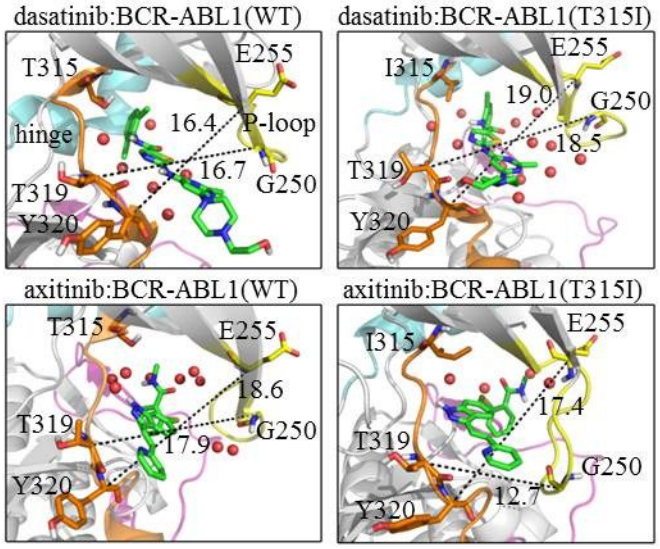


**Figure S1.** The representative structures of the energy minima of the free energy landscapes. The G250_Cα−T319_Cα distance and the E255_Cα−Y320_Cα distance are highlighted (unit is Å).

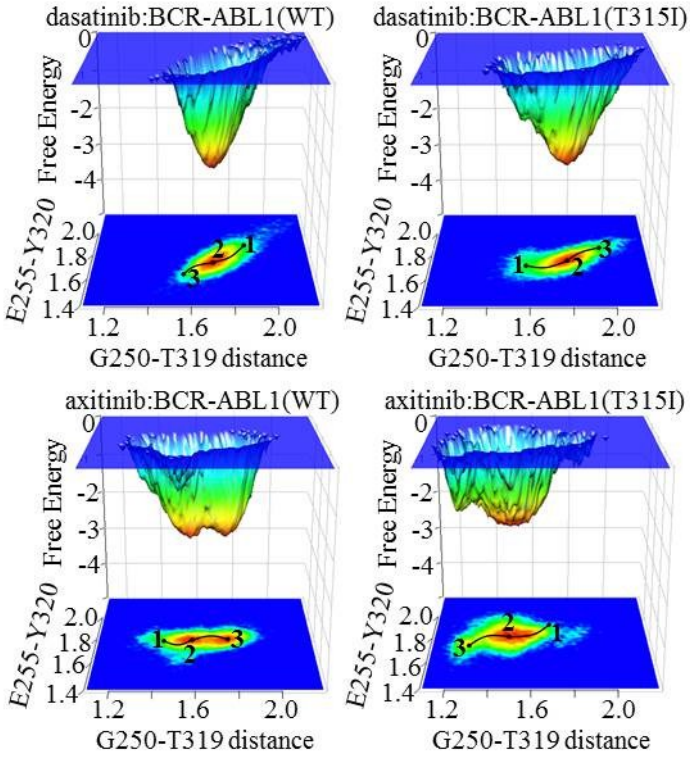


**Figure S2.** The free energy landscapes of the ligand:BCR-ABL1 complexes (DFG-in conformation) as a function of the G250_Cα−T319_Cα distance and the E255_Cα−Y320_Cα distance. G250 and E255 are located in P-loop, and T319 and Y320 are located in hinge. The distance unit is Å.

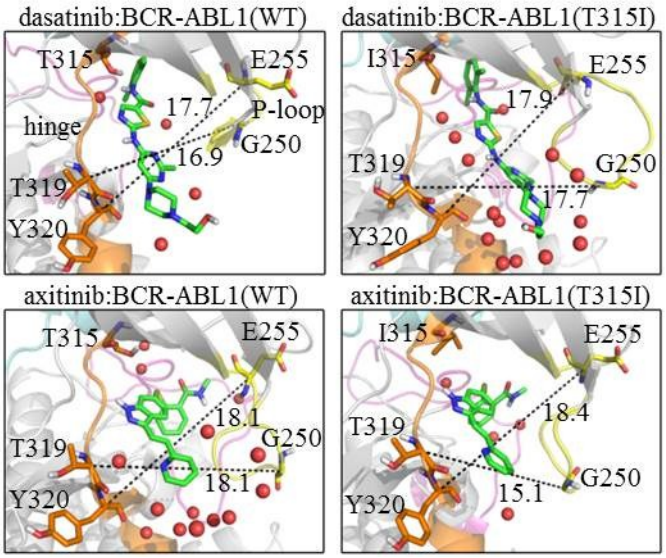


**Figure S3.** The representative structures of the energy minima of the free energy landscapes (BCR-ABL1 adopting DFG-in conformation). The G250_Cα−T319_Cα distance and the E255_Cα−Y320_Cα distance are highlighted (unit is Å).

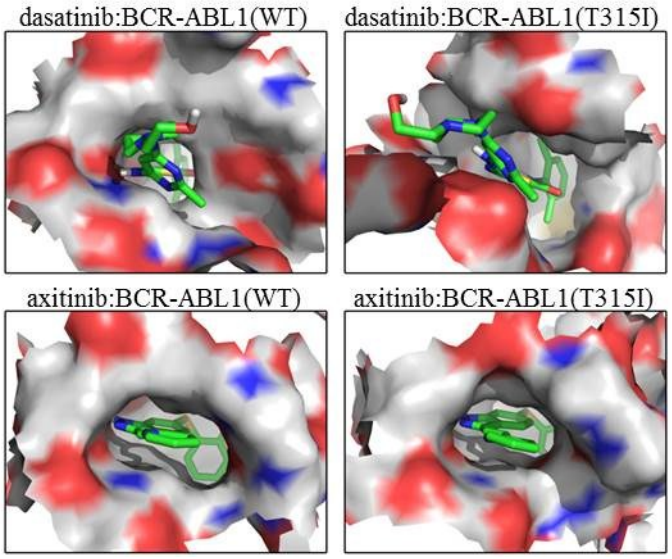


**Figure S4.** The surface representations of the binding site of ligand:BCR-ABL1 complexes (DFG-in conformation). Ligands are shown in sticks.

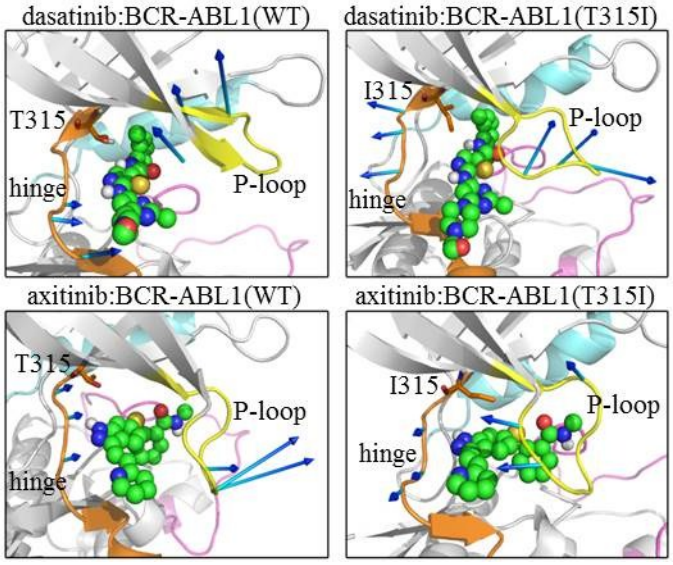


**Figure S5.** Collective motions corresponding to the PC1 for the ligand:BCR-ABL1 complexes (DFG-in conformation). The arrow presents the motion direction, and the arrow length describes the motion magnitude.

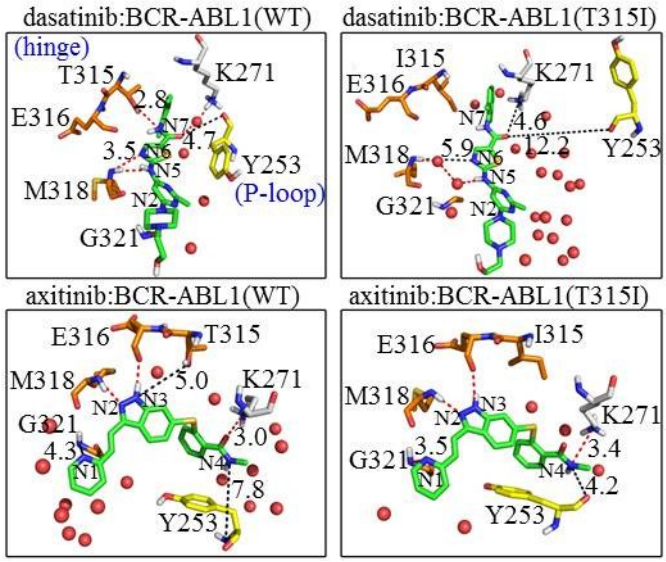


**Figure S6.** Interactions between ligands and their surrounding key residues for the representative structures of the energy minima of the free energy landscapes (BCR-ABL1 adopting DFG-in conformation). The residues colored in yellow are located in P-loop, while the residues colored in orange are located in hinge. The distance unit is Å.

**Table S1.** The hydrogen bonds between ligands and key residues of BCR-ABL1 kinases (DFG-in conformation)

| complex | donor | acceptor | Occupancy |
|---|---|---|---|
| **Dasatinib:BCR-ABL1(WT)** | K271-NZ-H | dasatinib-O | 20.43% |
| | T315-OG1-H | dasatinib-N7 | 65.57% |
| | M318-N-H | dasatinib-N6 | 52.52% |
| | M318-N-H | dasatinib-N5 | 20.19% |
| | G321-N-H | dasatinib-N2 | 0.48% |
| | dasatinib-N5-H | E316-O | 1.16% |
| | dasatinib-N5-H | M318-O | 44.90% |
| **Dasatinib:BCR-ABL1(T315I)** | K271-NZ-H | dasatinib-O | 6.48% |
| | I315 | dasatinib-N7 | 0% |
| | M318-N-H | dasatinib-N6 | 5.46% |
| | M318-N-H | dasatinib-N5 | 0.42% |
| | G321-N-H | dasatinib-N2 | 1.20% |
| | dasatinib-N5-H | E316-O | 0% |
| | dasatinib-N5-H | M318-O | 10.04% |
| **Axitinib:BCR-ABL1(WT)** | K271-NZ-H | axitinib-O | 29.61% |
| | T315-OG1-H | axitinib-N3 | 0.12% |
| | M318-N-H | axitinib-N2 | 98.98% |
| | M318-N-H | axitinib-N3 | 6.22% |
| | G321-N-H | axitinib-N1 | 47.68% |
| | axitinib-N4-H | Y253-O | 25.05% |
| | axitinib-N3-H | E316-O | 93.58% |
| | axitinib-N4-H | D381-OD1 | 10.86% |
| | axitinib-N4-H | D381-OD2 | 9.88% |
| **Axitinib:BCR-ABL1(T315I)** | K271-NZ-H | axitinib-O | 44.02% |
| | I315 | axitinib-N3 | 0% |
| | M318-N-H | axitinib-N2 | 98.90% |
| | M318-N-H | axitinib-N3 | 8.32% |
| | G321-N-H | axitinib-N1 | 44.06% |
| | axitinib-N4-H | Y253-O | 13.31% |
| | axitinib-N3-H | E316-O | 99.10% |
| | axitinib-N4-H | D381-OD1 | 15.49% |
| | axitinib-N4-H | D381-OD2 | 12.01% |

The hydrogen bonds are determined by the atoms distance between acceptor and donor <3.5Å and the angle between acceptor and H-donor >120°.

**Table S2.** Binding free energies of the ligand:BCR-ABL1 complexes (DFG-in conformation) calculated by MM-PBSA method (unit: kcal/mol).

| Energy items (kcal/mol) | Dasatinib:BCR-ABL1 (WT) | Dasatinib:BCR-ABL1 (T315I) | Axitinib:BCR-ABL1 (WT) | Axitinib:BCR-ABL1 (T315I) |
|---|---|---|---|---|
| $\Delta E_{ele}$ | -102.67±4.18 | -98.07±7.84 | -19.42±1.70 | -25.80±2.24 |
| $\Delta E_{vdw}$ | -55.58±0.10 | -51.31±1.97 | -44.86±0.86 | -46.21±1.59 |
| $\Delta E_{gas}$ | -158.25±4.21 | -149.37±8.60 | -64.28±1.68 | -72.00±2.28 |
| $\Delta G_{non\text{-}polar/PB}$ | -6.56±0.11 | -7.43±0.05 | -6.52±0.03 | -6.48±0.04 |
| $\Delta G_{polar/PB}$ | 126.06±3.68 | 132.21±7.17 | 34.81±1.59 | 40.43±1.96 |
| $\Delta G_{sol/PB}$ | 119.50±3.69 | 124.77±7.19 | 28.29±1.59 | 33.95±1.95 |
| $\Delta G_{bind}$ | -38.75±0.56 | -24.60±2.54 | -35.99±0.79 | -38.06±1.64 |

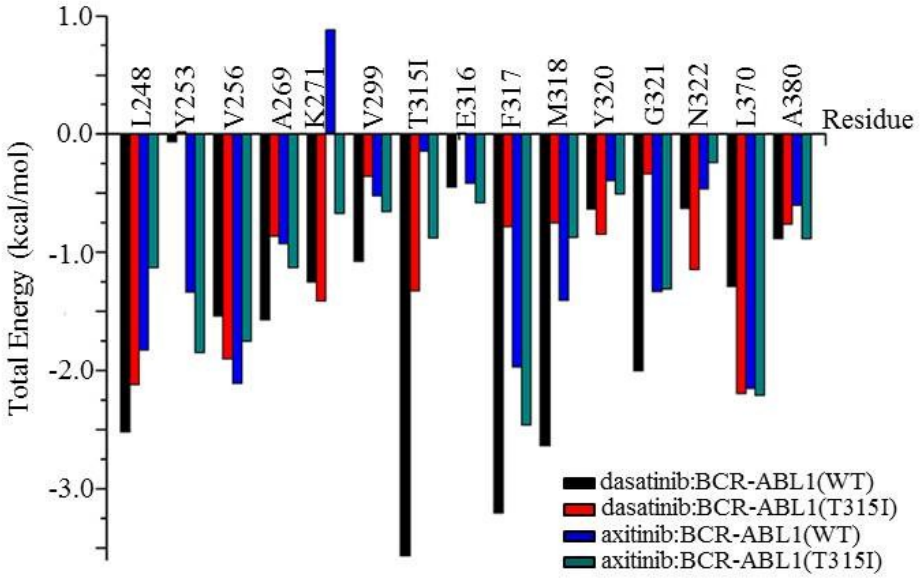


**Figure S7.** The contributions of the key residues for the ligand binding to BCR-ABL1 (DFG-in conformation) by MM-PBSA method.

**Table S3.** The residue-based decomposition analyses for the dasatinib:BCR-ABL1(WT) and dasatinib:BCR-ABL1(T315I) complexes (DFG-in conformation)

| | Dasatinib:BCR-ABL1(WT) | | | | Dasatinib:BCR-ABL1(T315I) | | | |
|---|---|---|---|---|---|---|---|---|
| Residue | $\Delta E_{ele}$ | $\Delta E_{vdw}$ | $\Delta G_{sol/PB}$ | $\Delta G_{bind}$ | $\Delta E_{ele}$ | $\Delta E_{vdw}$ | $\Delta G_{sol/PB}$ | $\Delta G_{bind}$ |
| L248 | -1.39 | -2.54 | 1.41 | -2.52 | -3.15 | -2.57 | 3.60 | -2.12 |
| Y253 | -0.25 | -0.18 | 0.36 | -0.07 | 0.51 | -0.02 | -0.48 | 0.02 |
| V256 | -1.67 | -1.24 | 1.37 | -1.54 | -1.89 | -1.49 | 1.48 | -1.91 |
| A269 | -0.11 | -1.53 | 0.07 | -1.57 | 0.23 | -1.01 | -0.08 | -0.86 |
| K271 | -30.53 | -1.83 | 31.11 | -1.26 | -16.14 | -1.32 | 16.05 | -1.41 |
| V299 | -0.16 | -0.84 | -0.08 | -1.08 | -0.84 | -0.22 | 0.70 | 0.36 |
| T315I | -6.55 | -1.66 | 4.64 | -3.57 | -0.55 | -1.44 | 0.66 | -1.33 |
| E316 | 5.36 | -0.53 | -5.28 | -0.45 | 4.75 | -0.18 | -4.56 | 0.01 |
| F317 | -1.64 | -2.09 | 0.52 | -3.21 | -0.04 | -0.68 | -0.08 | -0.79 |
| M318 | -6.56 | -2.01 | 5.94 | -2.64 | -1.12 | -1.11 | 1.48 | -0.75 |
| Y320 | 0.94 | -1.47 | -0.10 | -0.64 | -3.68 | -1.93 | 4.76 | -0.85 |
| G321 | -0.46 | -1.70 | 0.16 | -2.00 | -0.23 | -0.50 | 0.39 | -0.34 |
| N322 | -3.08 | -0.67 | 3.12 | -0.63 | -4.53 | -1.34 | 4.72 | -1.15 |
| L370 | -0.16 | -1.19 | 0.06 | -1.29 | -0.31 | -2.01 | 0.13 | -2.20 |
| A380 | -3.26 | -0.35 | 2.72 | -0.89 | -3.20 | -0.31 | 2.75 | -0.76 |

**Table S4.** The residue-based decomposition analyses for the axitinib:BCR-ABL1(WT) and axitinib:BCR-ABL1(T315I) complexes (DFG-in conformation)

| | Axitinib:BCR-ABL1(WT) | | | | Axitinib:BCR-ABL1(T315I) | | | |
|---|---|---|---|---|---|---|---|---|
| Residue | $\Delta E_{ele}$ | $\Delta E_{vdw}$ | $\Delta G_{sol/PB}$ | $\Delta G_{bind}$ | $\Delta E_{ele}$ | $\Delta E_{vdw}$ | $\Delta G_{sol/PB}$ | $\Delta G_{bind}$ |
| L248 | -0.25 | -1.85 | 0.27 | -1.83 | -0.30 | -1.19 | 0.35 | -1.13 |
| Y253 | -0.79 | -1.94 | 1.39 | -1.34 | -0.76 | -2.36 | 1.27 | -1.85 |
| V256 | -0.43 | -1.83 | 0.15 | -2.11 | -0.31 | -1.56 | 0.11 | -1.76 |
| A269 | -0.25 | -0.82 | 0.14 | -0.93 | -0.17 | -1.06 | 0.10 | -1.13 |
| K271 | -4.64 | 0.62 | 4.89 | -0.88 | -5.50 | -0.81 | 5.64 | -0.67 |
| V299 | 0.03 | -0.49 | -0.06 | -0.52 | 0.12 | -0.63 | -0.15 | -0.66 |
| T315I | 0.11 | -0.73 | 0.48 | -0.15 | 0.33 | -0.90 | -0.31 | -0.88 |
| E316 | -0.97 | -0.43 | 0.99 | -0.42 | -1.97 | 0.13 | 1.26 | -0.58 |
| F317 | -1.25 | -1.66 | 0.94 | -1.97 | -1.82 | -1.66 | 1.01 | -2.46 |
| M318 | -0.32 | -1.74 | 0.65 | -1.41 | 0.18 | -1.70 | 0.65 | -0.87 |
| Y320 | -0.21 | -0.51 | 0.32 | -0.40 | -0.36 | -0.53 | 0.38 | -0.51 |
| G321 | -0.33 | -1.27 | 0.26 | -1.33 | -0.32 | -1.20 | 0.21 | -1.31 |
| N322 | 0.30 | -0.39 | -0.37 | -0.47 | 0.25 | -0.31 | -0.18 | -0.24 |
| L370 | -0.26 | -2.06 | 0.17 | -2.15 | -0.22 | -2.15 | 0.16 | -2.21 |
| A380 | -0.18 | -0.55 | 0.13 | -0.60 | -0.28 | -0.77 | 0.16 | -0.89 |

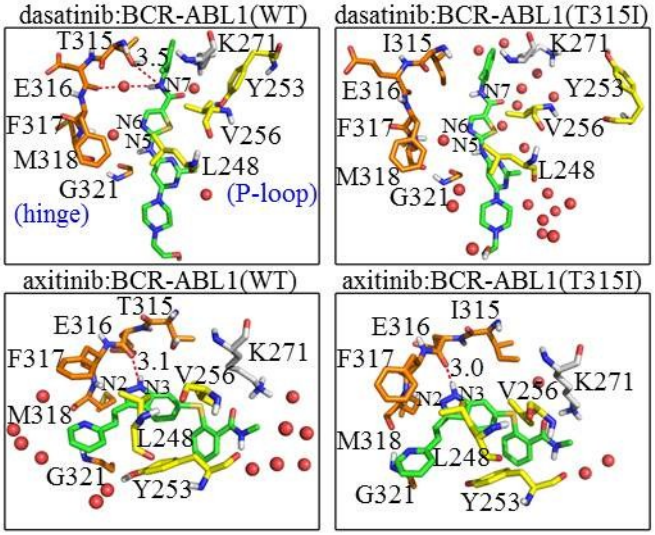


Figure S8. Interactions between the ligands and their surrounding residues of the final structure of the whole simulation (protein adopting DFG-in conformation). The distance unit is Å.

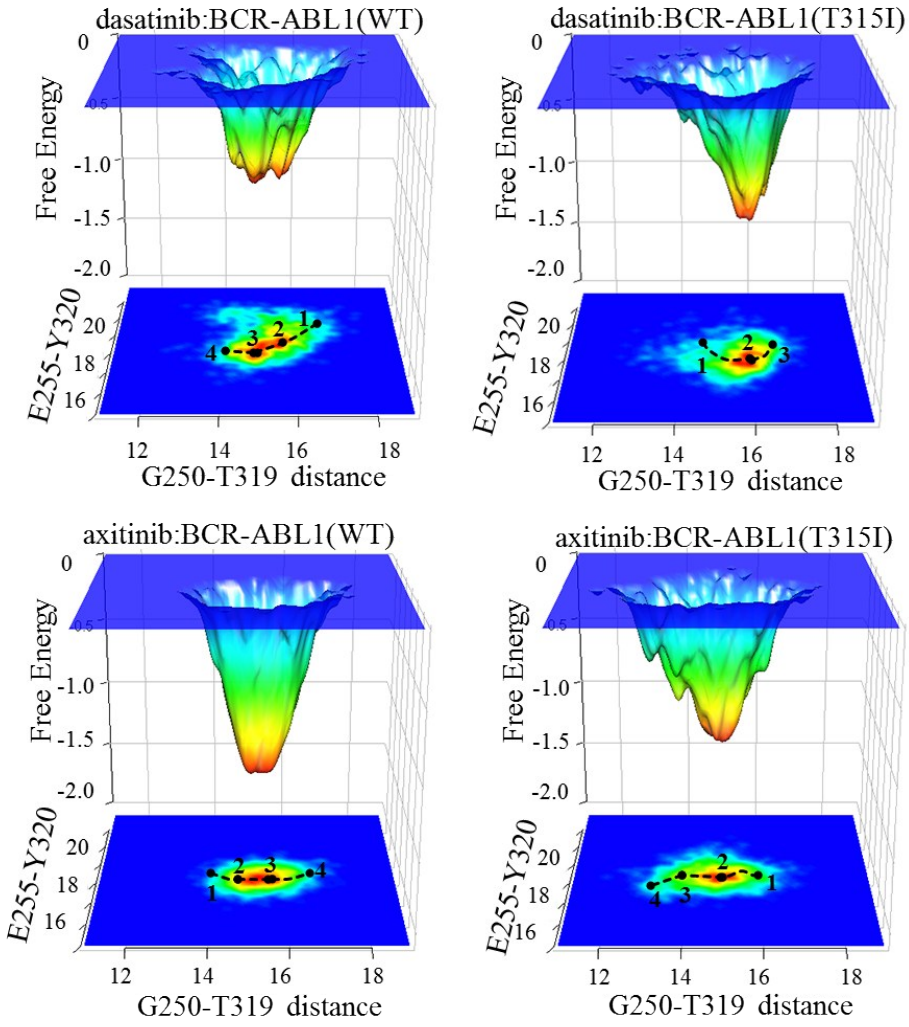


Figure S9. The free energy landscapes of the ligand:BCR-ABL1 complexes as a function of the G250_Cα−T319_Cα and E255_Cα−Y320_Cα distances for multiple short simulations..

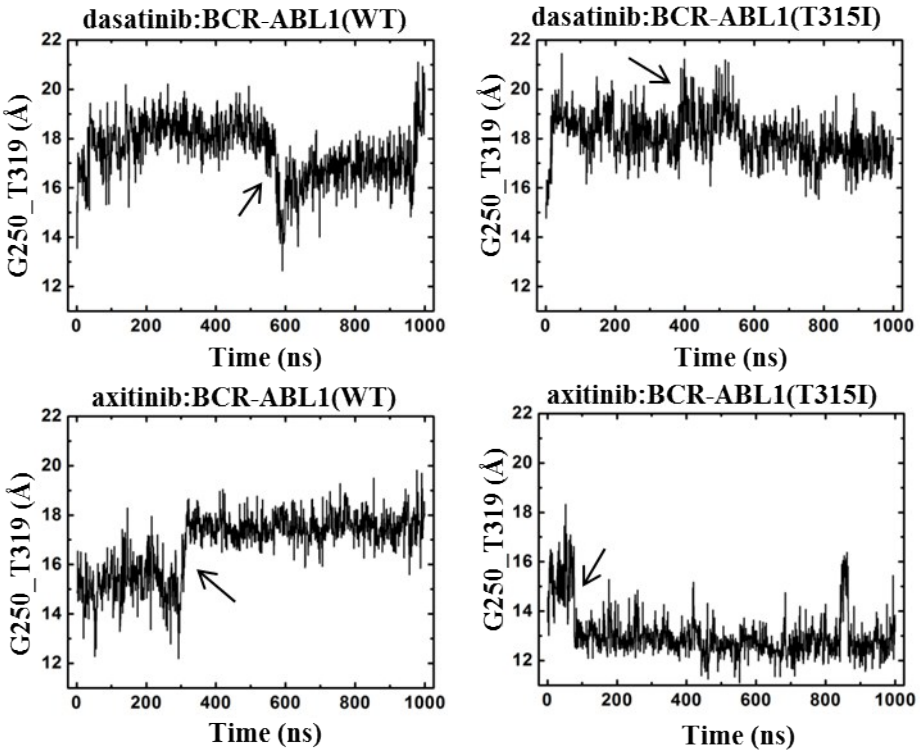


Figure S10. Time evolutions of G250_Cα−T319_Cα distances of the ligand:BCR-ABL1 complexes. The conformational changes are highlighted by arrows.